Josephson effect in *SNINS* and *SNIS* tunnel structures with finite transparency of the *SN* boundaries

A. A. Golubov and M. Yu. Kupriyanov

Moscow State University and the Institute of Solid State Physics, USSR Academy of Sciences
(Submitted 20 April 1989)
Zh. Eksp. Teor. Fiz. **96**, 1420–1433 (October 1989)

The proximity effect between a bulk superconductor and a thin layer of a normal metal is analyzed within the framework of a microscopic theory of superconductivity for the case of finite transparency of the *SN*-boundaries. The densities of states in the *N*-metal are found for a number of parameter values characterizing the boundary transparency (γ_B) and the proximity effect (γ_M). The conditions in which superconductivity suppression in the electrodes is negligible and calculation results are valid for high-temperature superconductor (HTSC) electrodes are determined. The critical (I_c) and quasiparticle currents in *SNINS* and *SNIS* tunnel junctions are calculated with different values of γ_B and γ_M. It is demonstrated that using HTSC electrodes in such structures makes it impossible to achieve optimum characteristic voltages V_c. The calculated $V_c(T)$ relations for the case where $\gamma_M \ll \gamma_B$ holds are in qualitative agreement with the experimental data obtained from studies of the intergrain boundaries in HTSC materials and explain the quantitative discrepancy between the experimental values of V_c and the estimates for ideal tunnel junctions with HTSC electrodes.

1. INTRODUCTION

The fabrication technology for Josephson tunnel structures based on ordinary "hard" superconductors is rather well developed today.[1,2] The dielectric interlayer in such junctions is produced by either oxidation of the lower electrode or by predeposition of a thin layer of another material, such as Al, onto the lower electrode. However attempts to carry over this technology for use in fabrication of junctions with high-temperature superconductor (HTSC) electrodes have encountered a number of difficulties. First, the high chemical activity of metal oxide superconductors facilitates chemical reactions at the HTSC boundary with both the conventional dielectrics used in microelectronics and virtually all normal metals, with the exception of Ag and Au (Refs. 3 and 4). Second, high-temperature annealing is accompanied by intense mutual diffusion[5] of the chemical elements in the dielectrics and the high-temperature superconductors, resulting in structural changes in a broad (of the order of 0.5 μm) boundary region. Such events have little effect on the critical temperature of HTSC-films of sufficient thickness (>0.5 μm), since metal oxide superconductors have a short coherence length. However they do play an essential role in the fabrication of tunnel junctions with HTSC electrodes. Indeed efforts to use the "natural" barrier at the boundaries of YBaCuO/Nb (Refs. 6 and 7), YBaCuO/Pb (Refs. 8 and 9), LaSrCuO/Pb (Ref. 10) as the dielectric interlayer were unsuccessful: The critical current of these junctions was zero at $T \sim 4.2$ K.

One escape from this situation lies in fabricating buffer layers of chemically less active materials such as Ag and Au between the HTSC-film and the dielectric layer. It has been proven experimentally that the use of Ag or Au buffer layers between the dielectric substrate and the HTSC-film not only limits the diffusion of the dielectric material into the HTSC-film but also causes texturing of the film,[5] while the poor diffusion of silver in, for example, YBaCuO, causes an increase in T_c of this compound.[11] Utilizing the Ag and Au layers in the YBaCuO/Au/A10_x/Nb (Ref. 12), YBaCuO/Ag/PbO_x/Pb (Ref. 13) tunnel structures made it possible to obtain junctions with a substantial critical current and a characteristic voltage $V_c > 0.04$ mV. However unlike the interface surface of ordinary metals, the YBaCuO/(Ag, Au) boundary has a finite resistance whose typical value lies in the range $R_b \sim 10^{-8}$–10^{-10} $\Omega\cdot\text{cm}^2$ (Refs. 13 and 14).

The current level of development of HTSC-materials technology therefore makes it possible to use such materials to fabricate tunnel *SNINS* or *SNIS'* junctions, where *S'* is an ordinary superconductor and the *SN* boundaries of such structures can have a random transparency. A complete theory of the Josephson effect in such structures does not yet exist even for the case of ordinary isotropic *S*- or *N*-metals. The purpose of the present study is to formulate such a theory and to determine the conditions in which superconductivity of the *S*-material will not be lost due to the proximity effect with the *N*-metal. When these conditions are satisfied the spatial variations in the superconducting properties of HTSC-electrodes are negligible. Moreover in spite of the significant spread of experimental values of the $2\Delta(T=0)/T_c$ ratio in metal oxide superconductors, the variation of $\Delta(T)$ with temperature is similar to that predicted by BCS theory. Hence the results derived in this case will also be valid for junctions with HTSC-electrodes.

2. JUNCTION MODEL AND ITS DESCRIPTION

We assume that one or both electrodes of the Josephson tunnel junction take the form of an *SN*-sandwich, while the insulating layer has such negligible transparency that it is possible to neglect the effect of the currents on the state of the electrodes. Moreover we assume that the dirty limit conditions hold for the *S*- and *N*-materials, the critical temperature of the *N*-material is equal to zero and the transverse dimensions of the junction are much less than the Josephson depth of penetration γ_J; all quantities can be assumed to depend solely on a single coordinate x normal to the interface surfaces of the materials. We will limit the analysis to the most important practical case

$$d_S \gg \xi_S, \quad d_N \ll \xi_N, \tag{1}$$

 0038-5646/89/100805-08$04.00 © 1990 American Institute of Physics

where $d_{N,S}$ and $\xi_{N,S}$ are the thicknesses and coherence lengths of the S- and N-metals. The first condition makes it possible to neglect the reduction in the critical temperature of the SN-electrode compared to the T_c of a bulk S-metal, while the second condition allows us to assume that all quantities within the N-layer are independent of x. In the ordinary relation of tunnel theory[15]

$$I=\mathrm{Re}\, I_p(\varepsilon)\sin\varphi+\mathrm{Im}\, I_p(\varepsilon)\cos\varphi+\mathrm{Im}\, I_q(\varepsilon),$$
$$\varphi=\varepsilon t+\varphi_0,\quad \varepsilon=2eV, \tag{2a}$$

$$\mathrm{Re}\, I_p(\varepsilon)=\frac{1}{2eR_0}\int_{-\infty}^{+\infty}\mathrm{th}\frac{\varepsilon'}{2T}[\mathrm{Im}\, F_1(\varepsilon')\,\mathrm{Re}\, F_2(\varepsilon'+\varepsilon)+\mathrm{Re}\, F_1(\varepsilon'+\varepsilon)\,\mathrm{Im}\, F_2(\varepsilon')]d\varepsilon'. \tag{2b}$$

$$\mathrm{Im}\, I_p(\varepsilon)=\frac{1}{2eR_0}\int_{-\infty}^{+\infty}\left[\mathrm{th}\frac{\varepsilon'+\varepsilon}{2T}-\mathrm{th}\frac{\varepsilon'}{2T}\right]\mathrm{Im}\, F_1(\varepsilon'+\varepsilon)\times\mathrm{Im}\, F_2(\varepsilon')d\varepsilon', \tag{2c}$$

$$\mathrm{Im}\, I_q(\varepsilon)=\frac{1}{2eR_0}\int_{-\infty}^{+\infty}\left[\mathrm{th}\frac{\varepsilon'+\varepsilon}{2T}-\mathrm{th}\frac{\varepsilon'}{2T}\right]N_1(\varepsilon'+\varepsilon)N_2(\varepsilon')d\varepsilon' \tag{2d}$$

this latter condition makes it possible to assume that the density of states $N(\varepsilon)$ and the functions $\mathrm{Im}\, F(\varepsilon)$, $\mathrm{Re}\, F(\varepsilon)$ are equal to their values at the SN-boundary, i.e., it is possible to neglect the low-probability electron tunneling processes from the bulk of the SN-electrode. In Eqs. (2) R_0 is the resistance of the junction in the normal state; φ is the phase difference of the order parameters of the electrodes: $\mathrm{Re}\, I_p(\varepsilon)$, $\mathrm{Im}\, I_p(\varepsilon)$, $\mathrm{Im}\, I_q(\varepsilon)$ is the Josephson supercurrent, the interferential current component and the quasiparticle current amplitudes, respectively; the indices 1 and 2 refer to the first and second electrodes.

As noted in Ref. 16 the problem of determining the functions $N(\varepsilon)$, $\mathrm{Im}\, F(\varepsilon)$, and $\mathrm{Re}\, F(\varepsilon)$ entering into (2) must be solved in two stages. It is first necessary to determine the spatial dependence of the order parameter in the SN-electrode $\Delta(x)$. Then after using this function it is necessary to solve the analytically-continued Usadel equations.

3. THE PROXIMITY EFFECT WITH RANDOM TRANSPARENCY OF THE *SN*-BOUNDARY

With these assumptions the proximity effect in a system of two "dirty" metals can be described within the framework of the equations (the domain $x\geqslant 0$ is occupied by the superconductor, while the domain $d_N\leqslant x\leqslant 0$ is occupied by the N-metal):

$$\left.\begin{aligned}&\Phi_S=\Delta+\xi_S^2\frac{\pi T_c}{\omega G_S}[G_S^2\Phi_S']' &&(3a)\\ &\Delta\ln(T/T_c)+2\pi\sum_\omega(\Delta-\Phi_S G_S)/\omega=0 &&(3b)\end{aligned}\right\}x\geqslant 0,$$

$$\left.\begin{aligned}&\Phi_N=\xi_N^2\frac{\pi T_c}{\omega G_N}[G_N^2\Phi_N']' &&(3c)\\ &G_{N,S}=\omega[\omega^2+\Phi_{N,S}^2]^{-1/2} &&(3d)\end{aligned}\right\}-d_N\leqslant x\leqslant 0,$$

where $\Phi_{N,S}$ are modified Usadel functions,[16] ω are the Mössbauer frequencies, Δ is the modulus of the order parameter, and the prime designates differentiation with respect to the coordinate x. Equations (3) must be supplemented by boundary conditions in the bulk of the S-electrode

$$\Phi_S(\infty)=\Delta(\infty)=\Delta(T), \tag{4}$$

as well as the N-metal-dielectric boundary ($x=-d_N$)

$$\Phi_N'(-d_N)=0 \tag{5}$$

and the N-metal-superconductor boundary ($x=0$)[17]

$$\xi_N\gamma_{BN}G_N\Phi_N'=G_S(\Phi_S-\Phi_N),\ \gamma_{BN}=R_b/\rho_N\xi_N, \tag{6a}$$
$$\xi_S G_S^2\Phi_S'=\gamma\xi_N G_N^2\Phi_N',\ \gamma=(\rho_S\xi_S)/(\rho_N\xi_N). \tag{6b}$$

Here $\Delta(T)$ is the absolute value of the order parameter of a homogeneous superconductor at T, $\rho_{N,S}$ are the resistivities of the N- and S-metals, while R_b is the product of the resistance of the NS-boundary and its area.

By virtue of the second inequality (1) we can neglect nongradient terms in Eq. (3c) in a first approximation in (d_N/ξ_N) and, by using (5), obtain in the next approximation

$$\Phi_N'(x)=\frac{\omega}{\pi T_c}\frac{\Phi_N(0)}{G_N(0)}\frac{x+d_N}{\xi_N^2}. \tag{7}$$

Determining $\Phi_N'(0)$ from (7) and substituting the resulting equation into conditions (6) we arrive at boundary conditions closed to the functions Φ_S

$$\xi_S G_S\Phi_S'(0)=\frac{\omega}{\pi T_c}\frac{\gamma_M\Phi_S(0)}{[1+\gamma_B^2\tilde\omega^2+2G_S\gamma_B\tilde\omega]^{1/2}},$$
$$\gamma_M=\gamma\frac{d_N}{\xi_N},\quad \gamma_B=\gamma_{BN}\frac{d_N}{\xi_N} \tag{8}$$

and a relation determining the functions Φ_N:

$$\Phi_N(x)=\frac{G_S(0)\Phi_S(0)}{[G_S(0)+\gamma_B\tilde\omega]},\quad -d_N\leqslant x\leqslant 0,\quad \tilde\omega=\frac{\omega}{\pi T_c}, \tag{9}$$

which are independent of the coordinate x to first order in d_N/ξ_N.

It follows from (8) and (9) that the problem of the proximity effect of a superconductor with a thin normal metal layer is reduced to solving Eqs. (3a, b) with the boundary conditions (4) and (8). This solution is simplified in a number of particular cases.

With small values of γ_M,

$$\gamma_M\ll(1+\gamma_B)(1-T/T_c)^{1/2}, \tag{10}$$

to lowest order in γ_M we have $\Phi_S'=0$ and the solution of equations (3a, b) reduces to

$$\Phi_S=\Delta_S=\Delta(T),\quad \Phi_N=\Delta(T)[1+\gamma_B(\omega^2+\Delta^2)^{1/2}/\pi T_c]^{-1}. \tag{11}$$

It follows from (11) that the values of the functions Φ_N decay monotonically and proportional to γ_B^{-1} with increasing γ_B in the range where $\gamma_B\gg 1$ holds.

Reversing the inequality (10)

$$\gamma_M\gg(1+\gamma_B)(1-T/T_c)^{1/2} \tag{12}$$

to first order in γ_M^{-1} the functions Φ_S in the immediate proximity of the SN-boundary ($0<x\ll\xi_S$) are equal to Ref. 18:

$$\Phi_S(x)=\Delta(x)=B(T)(x-d_N)/\xi_S,$$
$$B(T)=2T_c[1-(T/T_c)^2][7\zeta(3)]^{-1/2}. \tag{13}$$

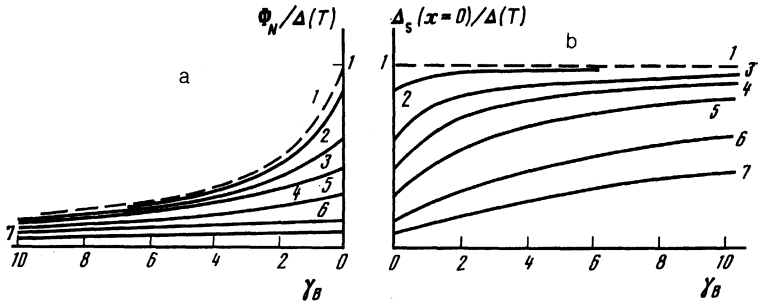

FIG. 1. The function Φ_N for $\omega = \pi T$ (a) and the order parameter in the S-region near the SN-boundary $\Delta_S(x=0)$ (b) plotted as a function of the transparency of the SN-boundary for various values of $\gamma_M = 0$; 0.1; 0.5; 1; 2; 5; 10 (curves 1; 2; 3; 4; 5; 6; 7, respectively).

In this approximation we obtain values independent of γ_B from (8), (9), and (12) for Φ_N:

$$\Phi_N = B(T)/\tilde{\omega}\gamma_M. \tag{14}$$

In the near-critical range of temperatures where $T \sim T_c$ holds, the Ginzburg-Landau equations are valid in the S-electrode. Determining the appropriate boundary conditions by the method discussed in Ref. 19 we obtain

$$\Phi_N = \frac{\Delta(T)}{(1+\gamma_B\tilde{\omega})(\alpha+(1+\alpha^2)^{1/2})} \qquad \alpha = \gamma_M \frac{\xi(T)}{2^{1/2}\xi_S} p, \tag{15}$$

where

$$p = \begin{cases} \frac{\gamma_B}{2}[\Psi(1/2+1/2\gamma_B)-\Psi(1/2)], & \gamma_M \ll \gamma_B+1, \\ [\gamma_B+7\zeta(3)/\pi^2]^{-1}, & \gamma_M \gg \gamma_B+1, \end{cases}$$

$\Psi(x)$ and $\zeta(x)$ are the digamma-function and zeta-function, respectively.

Numerical techniques were used to solve equations (3), (4), and (8) with random temperatures and values of γ_M and γ_B. The calculation results are given in Fig. 1 as plots of Φ_N ($\omega = \pi T$, $x = 0$) and $\Delta(x=0)$ as a function of the parameter γ_B for various values of γ_M.

The broken brace in Fig. 1 represents the asymptotic result derived from (9) corresponding to $\gamma_M = 0$:

$$\frac{\Phi_N(\omega=\pi T, \gamma_B)}{\pi T_c} = \frac{1}{\gamma_B+\pi/\gamma^*} \tag{16}$$

where $\gamma^* = 1.78$ is Euler's constant. As is evident from Fig. 1 with small values of the parameter γ_M the diminishing boundary transparency (i.e., the growth of the parameter γ_B) will result in a sharp drop in Φ_N characterizing the superconductivity induced in the N-layer. With large γ_M the function Φ_N has a weak dependence on barrier transparency all the way to $\gamma_B \sim \gamma_M$. When T is approximately equal to T_c we can easily see from (15) that the values of the functions Φ_N are in fact independent of γ_B when $\gamma_B < 1 + \gamma_M$ holds, and are determined by the temperature-dependent parameter $\Gamma_M = \gamma_M \xi_S(T)/\xi_S$. With large γ_B the finite transparency of the NS-boundary will result in additional suppression of Φ_N proportional to γ_B^{-1}. Therefore although the values of the functions Φ_S grow as the boundary transparency decreases ($\Phi_S \to \Delta(T)$ as $\gamma_B \to \infty$), the functions Φ_N decay monotonically, whence $\Phi_N \propto \gamma_B^{-1}$ when $\gamma_B > \max\{1, \gamma_M\}$ holds and they are virtually independent of γ_B for smaller values of this parameter and larger values of γ_M ($\gamma_M > 1$).

4. CALCULATION OF THE STATE DENSITIES

In calculating the state densities in equations (3) and boundary conditions (4) and (8) it is convenient to go over to new functions $\Phi = \omega \tan\theta$, $G = \cos\theta$ and to then carry out the substitution $\omega = -i\varepsilon$:

$$\xi_S^2\theta_S'' + i\tilde{\varepsilon}\sin\theta_S + \tilde{\Delta}(x)\cos\theta_S = 0, \tag{17}$$

$$\xi_S\theta_S'(0,\tilde{\varepsilon}) = -i\tilde{\varepsilon}\gamma_M \sin\theta_S(0,\tilde{\varepsilon})[1-\gamma_B^2\tilde{\varepsilon}^2-2i\tilde{\varepsilon}\cos\theta_S(0,\tilde{\varepsilon})]^{-1/2}, \tag{18a}$$

$$\theta_S(\infty,\tilde{\varepsilon}) = \operatorname{arctg}(i\tilde{\Delta}(T)/\tilde{\varepsilon}), \tag{18b}$$

where we have set $\tilde{\varepsilon} = \varepsilon/\pi T_c$, $\tilde{\Delta} = \Delta/\pi T_c$. From relation (9) for θ_N determining the desired functions,

$$N(\varepsilon) = \operatorname{Re}(\cos\theta_N), \quad \operatorname{Im} F(\varepsilon) = \operatorname{Im}(\sin\theta_N),$$

$$\operatorname{Re} F(\varepsilon) = \operatorname{Re}(\sin\theta_N)$$

we have the expression

$$\theta_N = \operatorname{arctg}\{\sin\theta_S(0,\tilde{\varepsilon})/[\cos\theta_S(0,\tilde{\varepsilon}) - i\tilde{\varepsilon}\gamma_B]\} \tag{19}$$

in which the functions $\theta_S(0,\tilde{\varepsilon})$ must be found from a solution of the boundary problem (17), (18) with the known function $\Delta(x)$.

The solution of this problem is simplified in the limit of small γ_M. Indeed the boundary condition (18a) reduces to $\theta_S'(0,\tilde{\varepsilon}) = 0$ when γ_M is equal to 0 and the boundary problem (17), (18) is satisfied by the solution (18b) which is independent of the coordinate x; substituting this solution into (19) we have

$$\sin\theta_N = \{1 - z^2[1+\beta(1-z^2)^{1/2}]^2\}^{-1/2},$$

$$z = \varepsilon/\Delta(T), \qquad \beta = \gamma_B\tilde{\Delta}(T), \tag{20}$$

$$\cos\theta_N = -iz[1+\beta(1-z^2)^{1/2}]\sin\theta_N. \tag{21}$$

It follows from (20), (21) that the desired state densities have two singularities for $z = 1$ and $z = z_0$, where

$$z_0 = -\frac{1}{3} + \frac{(\beta^2-3)^{1/2}}{3\beta}\begin{cases} [1+(A^2-1)^{1/2}]^{1/3}+[1-(A^2-1)^{1/2}]^{1/3}, & \beta \leqslant \beta_0, \\ 2\cos[1/3 \arccos A], & \beta \geqslant \beta_0, \end{cases} \tag{22}$$

$$A = \beta(18-\beta^2)/(\beta^2-3)^{3/2}, \quad \beta_0 = 11/2 + [1+(11/2)^2]^{1/2} \approx 11.09.$$

However the nature of the divergences is somewhat weaker than in BCS theory for a spatially-homogeneous superconductor:

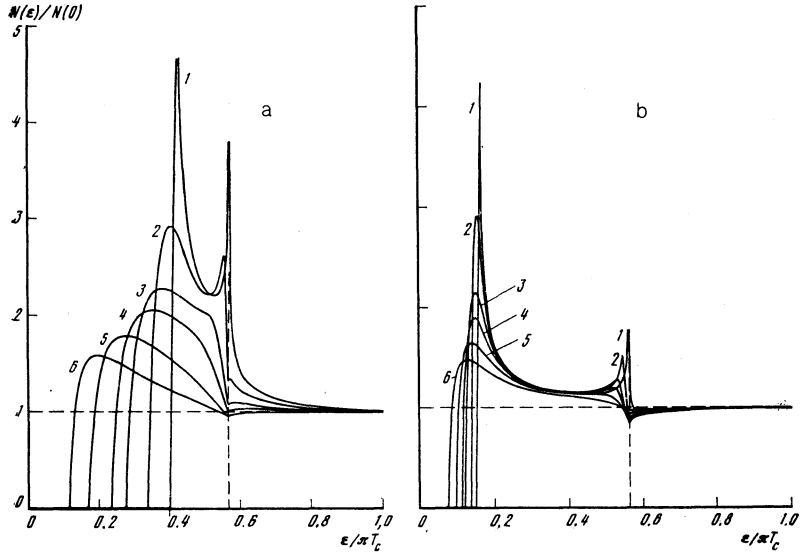

FIG. 2. The state density $N(\varepsilon)$ in the N-region of the SN-sandwich for $T \ll T_c$ (a—$\gamma_B = 1$; b—$\gamma_B = 5$) and various values of $\gamma_M = 0; 0.1; 0.3; 0.5; 1; 2$ (curves 1; 2; 3; 4; 5; 6, respectively). The vertical dotted line corresponds to $\varepsilon/\pi T_c = \Delta(0)/\pi T_c = \gamma^* \pi \approx 0.56$.

$$N(z)=\begin{cases} 0, & z<z_0, \\ \dfrac{z[1+\beta(1-z^2)^{1/2}]}{\{z^2[1+\beta(1-z^2)^{1/2}]^2-1\}^{1/2}}, & z_0<z<1, \\ \dfrac{z\{[(a^2+b^2)^{1/2}-a]^{1/2}+\beta(z^2-1)^{1/2}[a+(a^2+b^2)^{1/2}]^{1/2}\}}{(z^2-1)^{1/4}[2(a^2+b^2)]^{1/2}}, & z>1, \end{cases} \tag{23a}$$

$$\operatorname{Re} F(z)=\begin{cases} \{1-z^2[1+\beta(1-z^2)^{1/2}]^2\}^{-1/2}, & z<z_0, \\ 0, & z_0<z<1, \\ -\dfrac{[a+(a^2+b^2)^{1/2}]^{1/2}}{(z^2-1)^{1/4}[2(a^2+b^2)]^{1/2}}, & z>1, \end{cases} \tag{23b}$$

$$\operatorname{Im} F(z)=\begin{cases} 0, & z<z_0, \\ \{z^2[1+\beta(1-z^2)^{1/2}]^2-1\}^{-1/2}, & z_0<z<1, \\ \dfrac{[(a^2+b^2)^{1/2}-a]^{1/2}}{(z^2-1)^{1/4}[2(a^2+b^2)]^{1/2}}, & z>1, \end{cases} \tag{23c}$$

with $a = (z^2 - 1)^{1/2}(\beta^2 z^2 - 1)$, $b = 2\beta z^2$.

It is interesting to note that relations (23) correspond exactly to the results of McMillan's phenomenological tunnel theory of the proximity effect if we assume the following parameter values in this theory: $\Delta_N = 0$, $\Gamma_S = 0$, $\Gamma_N = \pi T_c/2\gamma_B$, i.e., if we go outside the limits of applicability of the model.[20]

Equations (17) and (18) were solved by numerical techniques with random values of ε and the parameters γ_M and γ_B. Figure 2 shows the state density relations for the SN-boundary when $T \ll T_c$ holds and for various values of γ_B and γ_M. It is clear that for $\gamma_M = 0$ the state densities have two singularities when $\varepsilon = \Delta(T)$ and $\varepsilon = z_0\Delta(T)$ hold, while the nature of the behavior of $N(\varepsilon)$ near these points will depend on γ_B. When γ_B is equal to 0, the parameter z_0 is equal to 1 and the regular expressions for the state densities of a homogeneous superconductor then follow from (23). The parameter z_0 drops below unity with increasing γ_B and two singularities appear in the state density. However the nature of the behavior of $N(z)$ is different in the neighborhood of these singularities:

$$N(z) = \begin{cases} \dfrac{1}{2}\beta^{-1/2}(z^2-1)^{-1/4}, & z=1+0, \\ 2^{-1/2}\beta^{-1/2}(1-z^2)^{-1/4}, & z=1-0, \\ (z-z_0)^{-1/2}\dfrac{z_0[1+\beta(1-z_0^2)^{1/2}](1-z_0^2)^{1/4}}{\{z_0[1+\beta(1-z_0^2)^{1/2}]+1\}^{1/2}[\beta+(1-z_0^2)^{1/2}-2\beta z_0^2]^{1/2}}, & z=z_0\pm 0. \end{cases} \tag{24}$$

It follows from (24) that the singularity is sharper for $\varepsilon = \Delta(T)$ $(z = 1)$ than for $\varepsilon = z_0\Delta(T)$, while its width decays in proportion to $\gamma_B^{-1/2}$ when γ_B exceeds unity at the same time that the width of the singularity in this limit is independent of γ_B when $\varepsilon = z_0\Delta(T)$ holds. The singularity shifts towards lower energies as the parameter γ_B increases when $\varepsilon = z_0\Delta(T)$ holds, and for $\gamma_B \gg 1$ we have $z_0 = \pi T_c/\Delta\gamma_B$. The quantity $z_0\Delta(T)$ is the energy gap in the elementary excitation spectrum in the N-area of the SN-sandwich.

The divergences in the state density are eliminated for $\gamma_M > 0$ for $z = z_0$ and $z = 1$. The function $N(z)$ has peaks of finite height at these energy values, as we see from Fig. 2, and the singularity smears more rapidly for $z = 1$ compared to the case when $z = z_0$ holds with an increasing parameter γ_M.

It is possible to estimate the height of the peak for $z = 1$ in the case where $\gamma_M \ll 1$ holds by using the first integral of Eq. (17) in the approximation $\Delta = \text{const}$ together with boundary condition (18) which yields the relation:

$$\gamma_M^2\tilde{\varepsilon}^2\sin^2\theta_S(0,\tilde{\varepsilon})/[1-\tilde{\varepsilon}^2\gamma_B^2-2i\tilde{\varepsilon}\gamma_B\cos\theta_S(0,\tilde{\varepsilon})]^{1/2} + (\tilde{\Delta}^2-\tilde{\varepsilon}^2)^{1/2}\sin\{\operatorname{arctg}[i\tilde{\varepsilon}/\tilde{\Delta}-\theta_S(0,\tilde{\varepsilon})]\} = (\tilde{\Delta}^2-\tilde{\varepsilon}^2)^{1/2}. \tag{25}$$

For the state density in the N-region we obtain from (19) and (25):

$$N(\varepsilon=\Delta)=\begin{cases} 1+1/\gamma_B\gamma_M^2\tilde{\Delta}, & \gamma_B \gg \gamma_M^{-2}, & (26a) \\ (3/4)^{1/2}(8\gamma_B/\gamma_M^4\tilde{\Delta})^{1/2}, & \gamma_M^4 \ll \gamma_B \ll \gamma_M^{-2}, & (26b) \\ 1/\gamma_M\tilde{\Delta}^{1/2}, & \gamma_B \ll \gamma_M^4. & (26c) \end{cases}$$

When $z = z_0$ the singularity will smear to a lesser degree with an increasing parameter γ_M. As is clear from the results of numerical calculations shown in Fig. 2 the singularity

evens out entirely with sufficiently large values of γ_M when $\varepsilon = \Delta(T)$ holds, and only the maximum when $\varepsilon = z_0\Delta(T)$ holds is conserved and we arrive at the results obtained previously in Ref. 16 in a model with a completely transparent *SN*-boundary ($\gamma_B = 0$). For γ_M, $\gamma_B \gg 1$ the energy gap in the *N*-region of the *SN*-sandwich

$$\Omega_0 \propto \min\{1/\gamma_M,\ 1/\gamma_B\},$$

and the maximum of the state density $N(\varepsilon)$ is smeared for $\varepsilon \sim \Omega_0$, while we have $N(\varepsilon) \to 1$ when $\varepsilon \gg \Omega_0$ holds and this function has no singularities.

It is important to note that the state densities obtained above entirely determine the voltage dependence of the differential conductivity of an *SNIN* tunnel junction $d(\operatorname{Im} I_q)dV \sim N(eV)$ at low temperatures ($T \ll T_c$).

Knowledge of the function Φ_N and the state densities in the *N* layer of the *NS* sandwich makes it possible to calculate the tunnel current in *SNINS*- and *SNIS'*-junctions.

5. STATIONARY PROPERTIES OF *SNINS*- AND *SNIS'*-STRUCTURES

The expression deriving from (2b) for the critical current of the tunnel junction is easily recast in the Matsubara representation:

$$I_c = \frac{2}{eR_0}\pi T \sum_{\omega>0} G_1(\omega)G_2(\omega)\Phi_1(\omega)\Phi_2(\omega)/\omega^2, \qquad (27)$$

where 1, 2 refer to first and second electrodes. For an *SNINS*-junction utilizing expressions (9) for the functions $\Phi_{1,2}$ we obtain

$$I_c = \frac{2}{eR_0}\pi T \sum_{\omega>0} \frac{\Phi_S^2(\tilde\omega)G_S^2(\tilde\omega)}{[1+\tilde\omega^2\gamma_B^2+2\tilde\omega\gamma_B G_S(\tilde\omega)]\tilde\omega^2}, \qquad (28a)$$

while for an *SNIS'*-junction we have

$$I_c = \frac{2}{eR_0}\pi T \sum_{\omega>0} \frac{\tilde\Delta'\Phi_S(\tilde\omega)G_S(\tilde\omega)}{(\tilde\omega^2+\tilde\Delta'^2)^{1/2}[1+\tilde\omega^2\gamma_B^2+2\tilde\omega\gamma_B G_S(\tilde\omega)]^{1/2}\tilde\omega}, \qquad (28b)$$

where $\tilde\Delta' = \Delta'/\pi T_c'$ holds, Δ' is the energy gap of the S'-electrode.

$\Phi_S = \Delta(T)$ is valid for $\gamma_M \ll 1$ and the asymptotic expressions for the critical current I_c of the *SNINS* junction follow from (28a) for $\gamma_B \gg 1$:

$$\frac{eR_0 I_c}{\pi T_c} = \begin{cases} \pi/2\gamma_B, & T \ll T_c, \\ \pi^2 T_c \Delta^2/48T^3\gamma_B^2, & \Delta/2T \ll 1, \end{cases} \qquad (29)$$

and for the *SNIS'* junction for $T \ll T_c$:

$$\frac{eR_0 I_c}{\pi T_c} = \ln(4\gamma_B\tilde\Delta')/\gamma_B, \qquad \gamma_B \gg 1/\tilde\Delta', \quad \tilde\Delta \gg \tilde\Delta'. \qquad (30)$$

It is clear that the $I_c(\gamma_B)$ relation for the *SNINS*-junction will be different for $T = 0$ and $T \sim T_c$, while at low temperatures the decay of I_c for the *SNIS'*-junction will be slower than for the *SNINS* junction.

With large values of the parameter γ_M ($\gamma_M \gg 1$) and using the solution (13), (14) for Φ_N we obtain asymptotic expression from (28a) for the critical current of the *SNINS*-junction

$$I_c = \frac{2\pi T}{eR_0}\frac{B^2(T)}{\gamma_M^2}\sum_{\omega>0}\frac{1}{\omega^4} = \frac{\pi^3 B^2(T)T_c^2}{48T^3 eR_0\gamma_M^2}, \qquad \gamma_M \gg T_c/T. \qquad (31)$$

With random values of γ_M, γ_B the critical current was determined numerically using the solutions found above for the functions Φ_N. Figure 3 provides numerical results for the $I_c(\gamma_B)$ relations for *SNINS* and *SNIS'* junctions for $T = 0$, where a superconductor with $T_c' = 0.1T_c$ was used as the S'-electrode. Moreover the temperature relations $\Delta_S(T)$ and $\Delta_S'(T)$ were used in the calculations together with the relation between $\Delta(T=0)$, $\Delta'(T=0)$ and T_c, T_c' which are valid within the framework of the BCS model.

As is clearly evident from the results shown in Fig. 3 the critical current of the junctions decays monotonically with increasing γ_B and for $\gamma_B > \max\{1,\gamma_M\}$ it converges on the asymptotic relations (29), (30). The nature of the variation of I_c with small values of γ_B is highly dependent on γ_M. For $\gamma_M \gg T_c/T$ the critical current is determined by relation (31) and is virtually independent of γ_B up through $\gamma_B \sim \gamma_M$. With small values of γ_M the diminishing transparency of the *SN*-boundary is accompanied by a sharp drop in I_c (in the range $0 < \gamma_B < 1$).

The absolute magnitude of critical current suppression is highly temperature-dependent. The $I_c(T)$ calculation results for *SNINS*- and *SNIS'*-junctions for $\gamma_B = 1$ and a variety of values of the parameter γ_M are given in Fig. 4. In the case where a normal interlayer is not present, i.e., in the case of the *SIS* junction for $\gamma_M = 0$, $\gamma_B = 0$ the $I_c(T)$ relation is determined by the Ambegaokar-Baratoff (AB) formula[21] and is represented by the dashed line in Fig. 4a. It is clear that in addition to the reduction in the absolute value of I_c the *N*-layer will produce a qualitative change in the nature of the $I_c(T)$ relation. Thus when $\gamma_M > \gamma_B$ holds

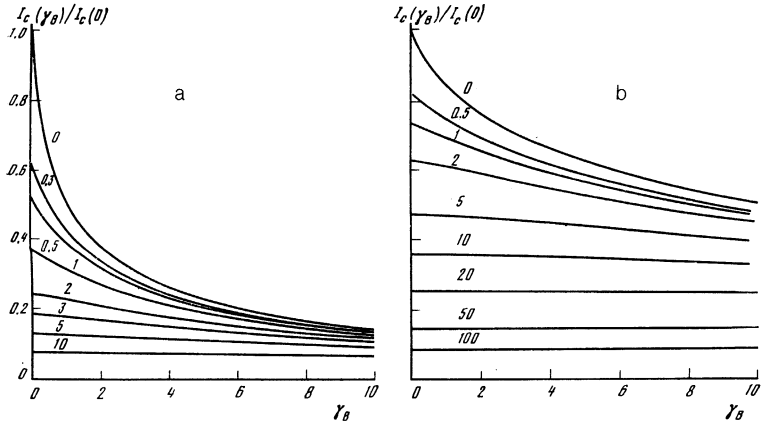

FIG. 3. Critical current plotted as a function of the transparency of the *SN*-boundary for different values of the parameter γ_M: a—*SNINS* junction; b—*SNIS'* junction; the numbers next to the curves represent the values of γ_M.

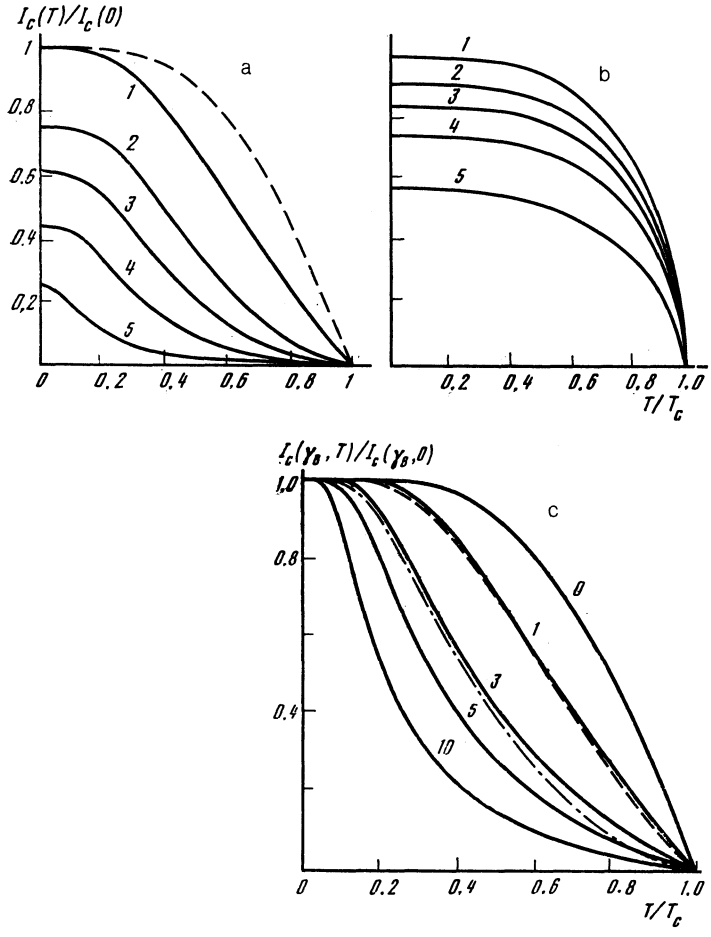

FIG. 4. The temperature dependence of the critical current for $\gamma_B = 1$ and various values of $\gamma_M = 0$; 0.5; 1; 2; 5; (curves 1; 2; 3; 4; 5, respectively): a—*SNINS* junction (the dotted line curve in *a* is the $I_c(T)$ relation for tunnel junctions[21]); b—*SNIS'* junction; c—$I_c(T)$ relation for $\gamma_M = 0$ and various values of γ_B (represented by the numbers labeling the curves); broken curve: Experimental data from Ref. 23; dot-dashed curve: From Ref. 22.

$I_c \sim (T_c - T)^2$ will be valid for the *SNIS*-junction near T_c, while $I_c \sim (T_c - T)^{3/2}$ will hold for the *SNINS*-junction at the same time that $I_c \sim (T_c - T)$ will be valid for the *SIS*-junction according to the AB theory. The form of the $I_c(T)$ relations indicated above can be attributed to the fact that when $T \approx T_c$ is valid the critical current is proportional to the product of the order parameters of the electrodes which depend on temperature either as $(T_c - T)^{1/2}$ in the absence of the proximity effect ($\gamma_M = 0$) or as $T_c - T$ when $\gamma_M > 0$ holds (Ref. 19). Therefore as we see from Fig. 4 the $I_c(T)$ relations for an *SNINS*-junction will have a positive slope at sufficiently high temperatures.

Small values of the parameter γ_M are of special interest. As noted above the values of the functions Φ_S at the *SN*-boundary coincide with $\Delta(T)$ for $\gamma_M \ll 1$, while the Φ_N functions which determine the level of the critical current in the *SNINS*-junction are represented as in (11). The $I_c(T)$ relations for various values of the parameter γ_B and calculated by formula (28) with $\Phi_S = \Delta(T)$ are shown in Fig. 4c. It is clear that the critical current level decays more rapidly at high temperatures $T \approx T_c$ with increasing γ_B in complete accordance with (29) compared to the range $T \ll T_c$. This serves to alter the nature of the relation $I_c(T)$ which goes from negative to positive slope over a broad temperature range beginning at $\gamma_B \sim 1$.

In this same figure the dashed line represents the experimental $I_c(T)/I_c(0)$ relations obtained in Refs. 23 and 22 from investigations of the critical current of the intergrain boundaries of HTSC-materials. It is clear that the experimental relations are in qualitative agreement with the calculated relations with values of $\gamma_B \approx 3$ (Ref. 22) and $\gamma_B \approx 1$ (Ref. 23). Since the values of γ_B obtained in this manner are greater than or equal to 1, then, as follows from (11), the values of the functions Φ_N and, consequently, the absolute values of the critical current will be approximately $1 + \gamma_B$

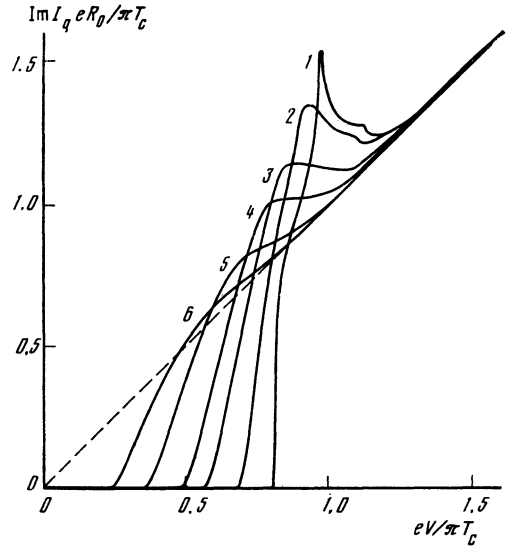

FIG. 5. I-V characteristics of the *SNINS* junction for $T = 0$; $\gamma_B = 1$ and various values of $\gamma_M = 0$; 0.1; 0.3; 0.5; 1; 2 (curves 1; 2; 3; 4; 5; 6, respectively).

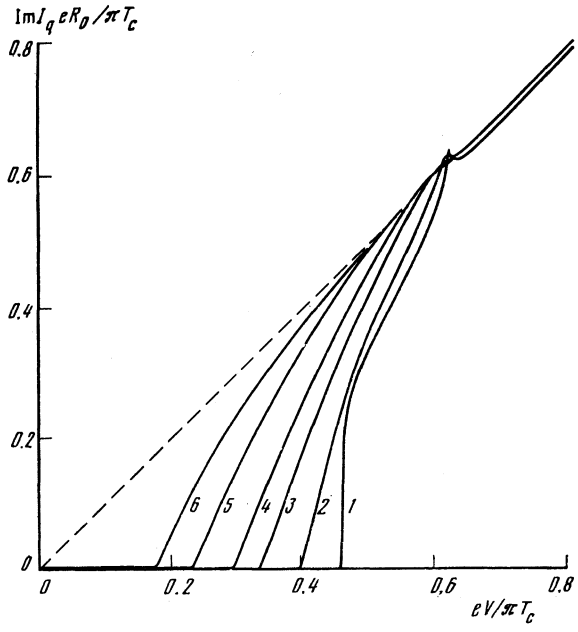

FIG. 6. I-V characteristics of the *SNIS'* junction for $T = 0$; $\gamma_B = 1$ and various values of $\gamma_M = 0$; 0.1; 0.3; 0.5; 1; 2 (curves 1; 2; 3; 4; 5; 6, respectively).

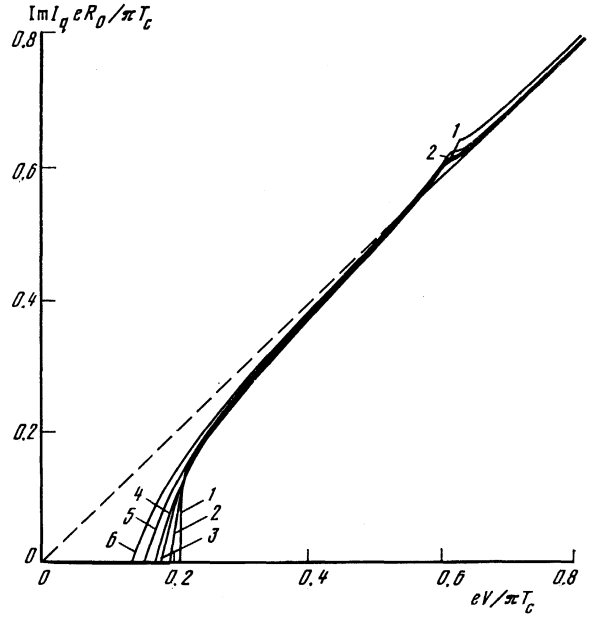

FIG. 8. I-V characteristics of the *SNIS'* junction for $T = 0$; $\gamma_B = 5$ and various values of $\gamma_M = 0$; 0.1; 0.3; 0.5; 1; 2 (curves 1; 2; 3; 4; 5; 6, respectively).

times lower than the values predicted by AB theory for $T \ll T_c$. It is this fact together with the effect of the finite thickness of the N-layer ($d_N \geqslant \xi_N$) that can explain the low experimental values of $I_c(0)$ compared to those predicted by AB theory for $2\Delta(0)/T_c = 3.5$.

One possible physical reason for the applicability of the proposed model to a description of the properties of the intergrain boundaries is the formation of poorly-conducting normal layers on atomic scales near the boundaries. The finite transparency of the intergrain boundaries is due to their sharpness on the interatomic scale.[23,24]

6. NONSTATIONARY PROPERTIES OF *SNINS*- AND *SNIS'*-STRUCTURES

Figures 5 and 6 present numerical results of the quasiparticle current Im $I_q(V)$ for *SNINS* and *SNIS'* junctions for $T = 0$, $\gamma_B = 1$ and for different values of γ_M. The I–V characteristics of the *SNINS* and *SNIS'* structures vary differently as the parameter γ_M increases. It is clear that unlike the results from standard tunnel theory[15] there is a sloping section in symmetrical junctions for $\gamma_M \leqslant 0.5$ instead of a current jump when $eV = 2\Delta$ holds; this section begins at the voltage $eV = 2z_0\Delta$ and terminates in a sharp singularity at

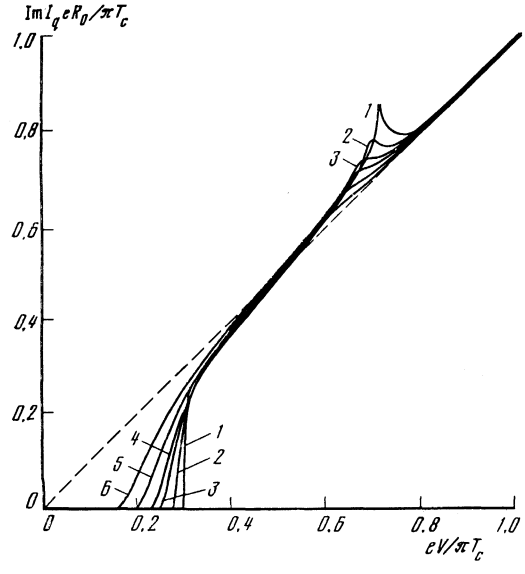

FIG. 7. I-V characteristics of the *SNINS* junction for $T = 0$; $\gamma_B = 5$ and various values of $\gamma_M = 0$; 0.1; 0.3; 0.5; 1; 2 (curves 1; 2; 3; 4; 5; 6, respectively).

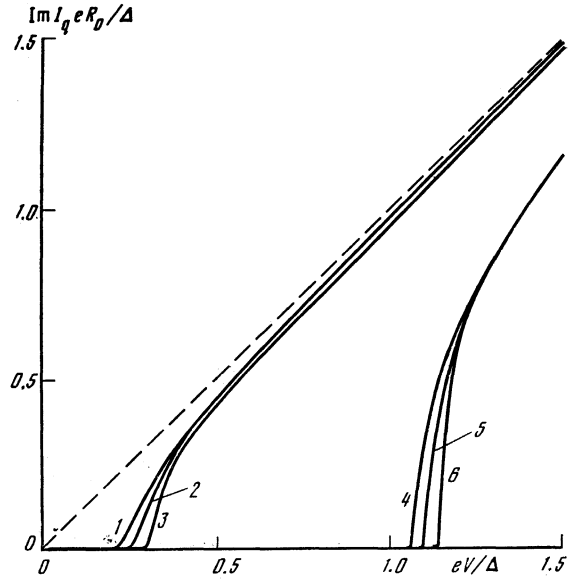

FIG. 9. I-V characteristics of the *SNINS* junction for $T = 0$; $\gamma_B = 100$ and values of $\gamma_M = 20$; 10; 5 (curves 1; 2; 3, respectively) and the *SNIS'* junction in the case $T_c' = 0.1T_c$ for $\gamma_M = 50$; 20; 5 (curves 4; 5; 6, respectively).

$eV = (z_0 + 1)\ \Delta$ which produces a kinked structure in the I-V characteristic. The singularity smoothes out with increasing growth of γ_M, while the Im $I_q(V)$ relation becomes linear. Moreover a weak singularity occurs with small values of γ_M for $eV = 2\Delta$. A sloping section occurs on the I–V characteristics of asymmetrical *SNIS'* junctions beginning at the voltage $eV = \Delta' + z_0\Delta$, and a weak, kinked singularity appears for small γ_M ($\gamma_M < 0.5$) for $eV = \Delta' + \Delta$; this singularity smears with increasing γ_M.

Figures 7 and 8 provide the Im $I_q(V)$ relations for *SNINS* and *SNIS'* junctions for $T = 0$, $\gamma_B = 5$. In this case the I-V characteristics of the *SNIS* and *SNIS'* junctions are qualitatively identical. The kinked structure when $eV = 2\Omega_0$ holds (Ω_0 is the gap width in the excitation spectrum of the *SN*-sandwich) does not exist in either case even when γ_M is equal to zero. Singularities appearing as peaks for $eV = (z_0 + 1)\Delta$ are found in the I–V characteristics of *SNINS* junctions together with the correspondingly weaker singularities for $eV = \Delta' + \Delta$ for the *SNIS'* junctions with small values of the parameter γ_M ($\gamma_M < 0.5$).

With large values of the parameters γ_B and γ_M ($\gamma_B \gg 1$ and $\gamma_M \gg 1$) the I–V characteristics of the *SNINS*- and *SNIS'*-structures in the low voltage range are shown in Fig. 9 for the case where $T = 0$. The structure appearing in the I–V characteristics at high voltages ($eV \gg \max\{1/\gamma_M,\ 1/\gamma_B\}$ holds for *SNINS* junctions and $eV - \Delta' \gg \max\{1/\gamma_M, 1/\gamma_B\}$ holds for *SNIS'* junctions) is completely smeared.

7. DISCUSSION OF RESULTS

The properties of *SNINS*- and *SNIS'*-tunnel structures with finite transparency of the *SN*-boundaries therefore differ substantially from the properties of both standard *SIS*-junctions and *SNINS* and *SNIS'* structures with transparent *SN*-boundaries. The nonzero resistances of the *SN*-boundary produce specific features in the I-V characteristics due to the complex structure of the electron state density in the *N*-layer of the compound *SN*-electrode and will also suppress the critical current of the junctions while reducing $V_c = I_c R_0$.

The latter fact makes *SNINS*- and *SNIS'*-structures with HTSC-electrodes rather unpromising for practical applications. Indeed an analysis of the experimental data on the surface resistance of the YBaCuO/Ag(Au) interface[13,14] yields $\gamma_B > 100$ and $\gamma_M > 10$. Such large values of γ_M and γ_B result in severe suppression of the critical current of the tunnel structures and make it impossible to achieve optimum values of V_c not only at liquid nitrogen but also at liquid helium temperatures. Moreover the slope of the I-V characteristics of such junctions in the gap voltage range is small compared to the analogous value in *SIS*-junctions employing ordinary superconductors.

However as suggested by the results obtained in Sec. 5 high-quality tunnel junctions based on HTSC materials can be fabricated by extracting from the polycrystalline film the tunnel structures formed by the natural boundaries of large superconducting grains.

[1]V. Keith and J. D. Leslie, Phys. Rev. B **18**, 4739 (1978).
[2]R. F. Broom, S. I. Raider, A. Oosenbrug *et al.*, IEEE Trans. Electr. Dev. **ED-27**, 1998 (1980).
[3]R. S. Williams and S. Chaudhary, *Chemistry of High Temperature Superconductors* II, Amer. Chem. Soc., Washington (1988).
[4]H. M. Meyer III, D. M. Hill, J. H. Weaver, and D. L. Nelson, *ibid.*, p. 280.
[5]C. X. Ren, G. L. Chen, and Y. Zheng, IEEE Trans. on Magnetics **25**, No. 2 (1989).
[6]Y. Katon, K. Tanabe, H. Asano, and O. Mishikami, Jap. J. Appl. Phys. **26**, L1777 (1987).
[7]M. G. Blamire, J. W. Morris, R. E. Sanekh, and J. B. Evetts, J. Phys. D **20**, 1330 (1987).
[8]I. Iguchi, H. Watanabe, Y. Kasai *et al.*, Jap. J. Appl. Phys. **26**, L645 (1987).
[9]A. Fournel, I. Oujia, J. P. Sorbier *et al.*, Europhys. Lett. **6**, 653 (1988).
[10]M. Naito, D. P. E. Smith, M. D. Kirk *et al.*, Phys. Rev. B **35**, 7228 (1987).
[11]Y. Nishi, S. Moriya, and S. Tokunaga, J. Mater. Science Lett. **7**, 596 (1988).
[12]A. Inone, K. Takeuchi, H. Ito *et al.*, Jap. J. Appl. Phys. **26**, L1443 (1987).
[13]K. Mizushima, M. Sagoi, T. Miura, and J. Yoshida, Jap. J. Appl. Phys. **27**, L1489 (1987).
[14]K. Mizushima, M. Sagoi, T. Miura, and J. Yoshida, Appl. Phys. Lett. **52**, 1101 (1988).
[15]N. R. Werthamer, Phys. Rev. **147**, 255 (1966).
[16]A. A. Golubov and M. Yu. Kupriyanov, J. Low Temp. Phys. **70**, 83 (1988).
[17]M. Yu. Kupriyanov and V. F. Lukichev, Zh. Eksp. Teor. Fiz. **94**, No. 6, 139 (1988) [Sov. Phys. JETP, **67**, 1163 (1988)].
[18]M. Yu. Kupriyanov and V. F. Lukichev, Fiz. Nizk. Temp. **8**, 1045 (1982) [Sov. J. Low Temp. Phys. **8**, 526 (1982)].
[19]A. A. Golubov, M. Yu. Kupriyanov, and V. F. Lukichev, Mikroelektronika **12**, 342 (1983).
[20]W. L. McMillan, Phys. Rev. **175**, 537 (1968).
[21]V. Ambegaokar and A. Baratoff, Phys. Rev. Lett. **10**, 486 (1963).
[22]C. W. Yuan, B. R. Zhao, Y. Z. Zhang *et al.*, J. Appl. Phys. **64**, 4091 (1988).
[23]J. Mannahart, P. Chaudhari, D. Dimos *et al.*, Phys. Rev. Lett. **61**, 219 (1988); **61**, 2476 (1988).
[24]H. W. Zandberger and G. Thomas, Acta Cryst. A **44**, 772 (1988).

Translated by Kevin S. Hendzel